# Theoretical and Experimental Modal Analysis of Multiple Flexible Disk-Flexible Shaft System

Naim Khader, Professor*; Ali Atoum, Graduate Student* and Ahmad Al-Qaisia, Associate Professor+
*Department of Mechanical Engineering, Jordan University of Science & Technology, P.O. Box 3030, Irbid 22100, Jordan.
*Department of Mechanical Engineering, University of Jordan, P. O. Box 13903, Amman 11942, Jordan

## ABSTRACT

The presented paper describes the results of an experimental study, carried out to determine the natural frequencies of a flexible shaft with several flexible disks. A single input single output approach was adopted to build the Frequency Response Function, with an impact hammer and a piezoelectric accelerometer used to excite the system and to record its response, respectively. The experimental results are compared with the corresponding results, obtained from a theoretical study, based on the assumed mode method, with the free vibration mode shapes of the system's individual components, i. e., flexible shaft and flexible disks, considered as the assumed functions. The acceptable agreement between the experimental and theoretical results provided confidence in the developed theoretical model. With the demonstrated confidence in the suggested theoretical model, it was further used to examine the effect of different rotor parameters, such as various shaft supporting conditions, disk-to-shaft bending rigidity ratio, span-wise position of the different disks along the shaft, as well as rotor speed, on the vibration characteristics of the examined rotor systems.

## INTRODUCTION

Flexible shafts with several flexible disks are found in turbines, compressors, and computer hard disk drives. It is important to accurately predict the natural frequencies of such systems to avoid resonant vibration during operation. Although it is a straightforward task to accurately predict the behavior of individual components, this is not good enough, because there high flexibility requirements introduces dynamic coupling between component modes, which might result in considerable difference between individual component and the complete system behavior. This subject has been investigated by several researches. Chong-Won Lee and Sang-Bok Chun [1] studied the effect of multiple flexible disks on the vibrational modes of a flexible shaft using assumed mode method. S.B. Chun and C.W. Lee [2] investigated the effect of the flexibility of a bladed disk assembly on the vibrational modes of a flexible rotor system by an analytical

substructure synthesis and assumed mode method. A. Shahab and J. Thomas [3] examined the effect of shaft flexibility on the dynamics characteristics of the disks, and the coupling effects between the shaft and disk modes. H. S. Jia, S.B. Chun and C.W. Lee [4] determined the natural frequencies and modes of the longitudinal coupled vibrations of a flexible shaft with multiple flexible disks by substructure synthesis. Chong-Won Lee and Jong-Seak Ham [5] studied the mode splits of the bending coupled modes of a rotating shaft with multiple flexible disks. I.Y. Shen and C.P.R. Ku [6] studied natural frequencies and mode shapes of spinning disk/spindle assembly, consisting of multiple elastic circular plates mounted on a rigid spindle that undergoes infinitesimal rigid-body translation and rotation. F. Wu and G.T. Flowers [7] developed a procedure to account for disk flexibility, which can be used to investigate how such effects might influence the natural frequencies and critical speed of practical rotors. C.W. Lee, H.S. Jia, C.S. Kim and S.B. Chun [8] presented a method to calculate the natural frequencies of the complicated coupled vibration of hard disk drive HDD spindle system (flexible shaft-multiple flexible disk systems), both the longitudinal and bending coupled vibration are included. Jr. Yi shen, Chaw-Wu Tseng and I.Y. shen [9] studied a rotating spindle carrying multiple flexible disks mounted on a flexible housing/stator assembly throughout ball bearing. G.H. Jang, S.H. Lee and M.S. Jung [10] analyzed the free vibration of a spinning flexible disk-spindle system supported by ball bearing and flexible shaft. Seungchul Lim [11] studied the flexural vibration of the hard disk drive spindle system
The presented work was intended to expand our experience in this field [12-14 ] by accounting for multiple flexible disks in the theoretical model on one side, and by experimentally verifying the obtained theoretical results. Equations of motion for the multiple flexible disk-flexible shaft were derived using the assumed mode method, with individual component modes used as the assumed functions. The resulting eigenvalue problem was solved to determine the natural frequencies of the coupled disk-shaft system for a wide range of rotor speed and different shaft-disk combinations.
The influence of disk-to-shaft bending rigidity ratio on the interaction between individual shaft and disk modes was examined. Several disk-shaft combinations were designed and built. Their natural frequencies were calculated from theory and experiment. An impact hammer was used to excite the system, and a piezoelectric accelerometer was fixed to one of the disks to obtain the response. The LabView software was used to acquire excitation and response signals, and to build the Frequency Response Function, which provides the desired frequency information.

## THEORETICAL MODAL ANALYSIS

**Model description:**
The examined rotor consists of a number of flexible disks $N_d$ attached to a either simply supported or fixed-free flexible shaft. The shaft is modeled by a slender beam with circular cross section and uniformly distributed mass and stiffness. Each of the flexible disks is modeled by an annular thin plate, with uniformly distributed mass and bending rigidity, and clamped at its inner radius to the shaft, as shown in figure 1.

**Equations of motion:**
The considered continuous multiple flexible disk-flexible shaft structure is discretized by application of the assumed mode method, where the flexible deformation of the disk or shaft is represented by summation of a number of time-dependent generalized coordinates, multiplied by assumed functions. The mode shapes of individual flexible disk or flexible shaft are taken as the assumed functions.

This method is combined with Lagrange's equation $\frac{d}{dt}\left(\frac{\partial L}{\partial \dot{q}_j}\right)-\left(\frac{\partial L}{\partial q_j}\right)=0$, to derive the governing equations of motion for the complete system, where $L=(T-U)$ and $q_j$, $T$, $U$ are the j-th generalized coordinate, total kinetic energy and total strain energy, respectively.

**Kinetic energy:**
Figure 2 shows a flexible shaft-disk system in deformed position, with three coordinate systems: Attached to the disk or shaft cross section system $X_2Y_2Z_2$, fixed in space system XYZ, and an intermediate system $X_1Y_1Z_1$. The position vector of an arbitrary disk or shaft element in the nonrotating undeformed position is defined by its spanwise *z*, radial r, and angular , positions. In the adopted structural model, the centerline of the shaft is allowed to bend by $U_s(z,t)$ and $V_s(z,t)$ along *X* and *Y* axes of the fixed in-space system, which results in tilting of the shaft's

cross-section by $\Theta_{sx}(z,t)=\dfrac{\partial V_s(z,t)}{\partial z}$ and $\Theta_{sy}(z,t)=\dfrac{\partial U_s(z,t)}{\partial z}$ about the same axes, respectively. Due to bending of the shaft's centerline and tilting of its cross-section, the i-th disk will have two rigid body translations $U_{di}=U_s(z_i,t)$ and $V_{di}=V_s(z_i,t)$, and two rigid body rotation $\Theta_{dxi}=\Theta_{sx}(z_i,t)$ and $\Theta_{dyi}=\Theta_{sy}(z_i,t)$, along and about *X* and *Y* axes, respectively, where $z_i$ is the span wise position of the i-th disk along the shaft,. In addition to its rigid body translations and rotations due to shaft bending, the disk has the transverse deformation $w(r,\theta,t)$. During rotation at a constant angular speed $\Omega$, the position vector for any disk or shaft element in the rotating and deformed position, is given in an attached to cross section coordinate system $X_2Y_2Z_2$ by $\{r\cos\Psi \quad r\sin\Psi \quad w\}^T$, where $\Psi=\theta+\Omega t$. Through the appropriate coordinate transformation, the position vectors of disk $\{X\}_{di}$ and shaft $\{X\}_s$ elements can be expressed in the fixed in-space system as:

$$\{X\}_{di}=\left|\begin{matrix} U+r\cos\Psi+w\cos\Theta_x\sin\Theta_y \\ V+r\sin\Psi+w\sin\Theta_x \\ w-r\sin\Psi\sin\Theta_x-r\cos\Psi\sin\Theta_y \end{matrix}\right|_{di} \tag{1}$$

$$\{X\}_s=\left|\begin{matrix} U+r\cos\Psi \\ V+r\sin\Psi \\ -r\sin\Psi\sin\Theta_x-r\cos\Psi\sin\Theta_y \end{matrix}\right|_s \tag{2}$$

A suitable form to derive the following expression for the kinetic energy of the i-th disk $T_{di}$, and of the shaft $T_s$.

$$\begin{aligned} T_{di}=\frac{1}{2}\rho_d h_d \int_r\int_\theta [(\dot{U}_s^2+\dot{V}_s^2-2r\Omega\sin\Psi w\dot{\Theta}_{dx}+2\Omega r\cos\Psi w\dot{\Theta}_{dy}+\Omega^2r^2+\dot{w}^2 \\ -2r\sin\Psi\dot{\Theta}_{dx}\dot{w}-2r\cos\Psi\dot{\Theta}_{dy}\dot{w}+r^2\sin^2\Psi\dot{\Theta}_{dx}^2+r^2\cos^2\Psi\dot{\Theta}_{dy}^2 \\ -2r^2\Omega\sin^2\Psi\dot{\Theta}_{dx}\Theta_{dy}+2r^2\Omega\cos^2\Psi\Theta_{dx}\dot{\Theta}_{dy})rdrd\theta]_{di} \end{aligned} \tag{3}$$

$$\begin{aligned} T_s=\frac{1}{2}\rho_s\int_0^L\int_A \dot{U}^2+\dot{V}^2+\Omega^2r^2+r^2\sin^2\Psi\dot{\Theta}_{sx}^2+r^2\cos^2\Psi\dot{\Theta}_{sy}^2 \\ -2r^2\Omega\sin^2\Psi\dot{\Theta}_{sx}\Theta_{sy}+2r^2\Omega\cos^2\Psi\Theta_{sx}\overset{*}{\Theta}_{sy})dAdz \end{aligned} \tag{4}$$

The total kinetic energy of the system will be $T=T_s+\sum_{i=1}^{ND}T_{di}$. Detailed derivations are given in [15].

**Strain energy:**
The strain energy of the rotating flexible disk consists of tow parts. Strain energy due to pure bending and strain energy due to the additional stretching of the middle plane, caused by its deformation $w(r,\theta,t)$ in the presence of in-plane centrifugal stresses, associated with disk rotation. Thus, $U_d=U_{d1}+U_{d2}$, where $U_{d1}$ is the strain energy associated with transverse deformation, and $U_{d2}$ is associated with centrifugal stiffening due to rotation.

$$\{U_{d1}\}_i = (\frac{D_d}{2}\int_r\int_\theta[(\nabla^2 w)^2 - 2(1-\nu)\frac{\partial^2 w}{\partial r^2}(\frac{1}{r}\frac{\partial w}{\partial r}+\frac{1}{r^2}\frac{\partial^2 w}{\partial r^2}) + 2(1-\nu)(\frac{\partial}{\partial r}(\frac{1}{r}\frac{\partial w}{\partial \theta}))^2]rdrd\theta)_{di} \tag{5}$$

$$\{U_{d2}\}_i = (\frac{1}{2}h_d\int_r\int_\Theta[\sigma_r(\frac{\partial w}{\partial r})^2 + \sigma_\theta(\frac{\partial w}{r\,\partial\theta})^2]rdrd\theta)_{di} \tag{6}$$

Where $\sigma_r$ and $\sigma_\theta$ are normal stress resultants, given in details in [15].
The strain energy of the flexible shaft is given by:

$$U_s = \frac{E_s I_s}{2}\int_0^L\left\{(\frac{\partial^2 U_s}{\partial z^2})^2 + (\frac{\partial^2 V_s}{\partial z^2})^2\right\}dz \tag{7}$$

The total kinetic and strain energy of the considered system will be:

$$\begin{aligned} T &= T_s + \sum_{i=1}^{ND} T \\ U &= U_s + \sum_{i=1}^{ND}(U_{d1}+U_{d2})_i \end{aligned} \tag{8}$$

**Discretization of the system:**
The assumed mode method is employed to discretize the system, by assuming the flexible deformations of the shaft disk system as a summation of a number of unknown generalized coordinates multiplied by known assumed functions, i. e. ,

$$U_s(z,t) = \sum U_m(z)a_m(t) \tag{9}$$

$$V_s(z,t) = \sum V_m(z)b_m(t) \tag{10}$$

$$\Theta_{sx}(z,t) = \sum V'_m(z)b_m(t) \tag{11}$$

$$\Theta_{sy}(z,t) = \sum U'_m(z)a_m(t) \tag{12}$$

Where $a_m$ and $b_m$ are the generalized coordinates, and $U_m$ and $V_m$ are the mode shapes of the transverse free vibration of the shaft alone, considered as the assumed functions.
Similar expressions can be written for the flexible disk deformations. However, it must be emphasized here that only one nodal diameter disk modes couple with shaft deformation, therefore, only these one nodal diameter disk modes are considered in the assumed mode method, and the disk flexible deformation is assumed in the following form:

$$w(r,\theta,t) = \sum_m\left[w_m(r)\sin\theta\, q_{ms}(t) + w_m(r)\cos\theta\, q_{mc}(t)\right] \tag{13}$$

Where $q_{ms}$ and $q_{mc}$ are the generalized coordinates, and $W_m$ is the m-th mode shape of the transverse free vibration of the disk alone, considered as the assumed function.

If the non-dimensional parameters

$$\overline{\Omega}^2 = \frac{\Omega^2}{(E_s I_s / M_s L_s^{\ 3})}; \qquad \beta = \frac{(D_d / R_d^2)_i}{(E_s I_s / L^3{}_s)}; \qquad \mu_d = \frac{M_d}{M_s}; \qquad \bar{r} = \frac{r}{R_d}; \qquad \widetilde{R}_d = \frac{R_d}{L_s};$$

$\widetilde{R}_s = \dfrac{R_s}{L_s}$; $\widetilde{k}_d = \sqrt{\left(\dfrac{I}{AR}\right)_d}$; $\widetilde{k}_s = \sqrt{\left(\dfrac{I}{AR}\right)_s}$ and $\bar{z} = \dfrac{z}{L_s}$, are introduced in the modal expressions of the flexible disk and shaft deformations, then the total potential and kinetic energy expressions can be given by:

$$\begin{aligned}
T &= \sum T_d + T_s \\
&= \frac{1}{2}\sum_K \mu\Big(\sum_m \sum_n (U_m U_n \dot{a}_m \dot{a}_n + V_m V_n \dot{b}_m \dot{b}_n \ \text{-} 2\widetilde{R}_d \overline{\Omega} U'_m \dot{a}_m q_{ns} \int w_n \bar{r}^2 d\bar{r} \\
&\quad + 2\widetilde{R}_d \overline{\Omega} V'_m \dot{b}_m q_{nc} \int w_n \bar{r}^2 d\bar{r} + \dot{q}_{mc} \dot{q}_{nc} \int w_m w_n \bar{r} d\bar{r} + \dot{q}_{ms} \dot{q}_{ns} \int w_m w_n \bar{r} d\bar{r} \\
&\quad \text{-} 2\widetilde{R}_d V'_m \dot{b}_m \dot{q}_{ns} \int w_n \bar{r}^2 d\bar{r} \ \text{-} 2\widetilde{R}_d U'_m \dot{a}_m \dot{q}_{nc} \int w_n \bar{r}^2 d\bar{r} + \widetilde{k}_d^{\ 2} \widetilde{R}_d^{\ 2} V'_m V'_n \dot{b}_m \dot{b}_n \\
&\quad + \widetilde{k}_d^{\ 2} \widetilde{R}_d^{\ 2} U'_m U'_n \dot{a}_m \dot{a}_n \ \text{-} 2\overline{\Omega}\widetilde{k}_d^{\ 2} \widetilde{R}_d^{\ 2} U'_m V'_n a_m \dot{b}_n + 2\overline{\Omega}\widetilde{k}_d^{\ 2} \widetilde{R}_d^{\ 2} U'_m V'_n \dot{a}_m b_n) + \overline{\Omega}^2 I_p \Big)_{dk} \\
&\quad + \frac{1}{2}\sum_m \sum_n [\dot{a}_m \dot{a}_n \int_0^1 U'_m U'_n d\bar{z} + \dot{b}_m \dot{b}_n \int_0^1 V'_m V'_n d\bar{z} + \widetilde{k}_s^{\ 2} \widetilde{R}_s^{\ 2} \dot{a}_m \dot{a}_n \int_0^1 U'_m U'_n d\bar{z} \\
&\quad + \widetilde{k}_s^{\ 2} \widetilde{R}_s^{\ 2} \dot{b}_m \dot{b}_n \int_0^1 V'_m V'_n d\bar{z} \ \text{-} 2\overline{\Omega}\widetilde{k}_s^{\ 2} \widetilde{R}_s^{\ 2} a_m \dot{b}_n \int_0^1 U'_m V'_n d\bar{z} + 2\overline{\Omega}\widetilde{k}_s^{\ 2} \widetilde{R}_s^{\ 2} \dot{a}_m b_n \int_0^1 U'_m V'_n d\bar{z}]
\end{aligned} \tag{14}$$

$$U = \sum (U_{d1} + U_{d2})_i + U_s \tag{15}$$

$$\begin{aligned}
U &= \sum_k \Bigg\{ \sum_m \sum_n \Bigg\{ \frac{\beta}{2} \int (w''_m w''_n \bar{r} + 2\nu w''_m w'_n - \frac{2\nu}{\bar{r}} w''_m w_n + \frac{3-2\nu}{\bar{r}} w'_m w'_n - \frac{6-4\nu}{\bar{r}^2} w'_m w_n + \frac{2(1-\nu)}{\bar{r}^3} w_m w_n d\bar{r}) \\
&\qquad + \frac{\mu}{2}\overline{\Omega}^2 \int_{\bar{r}} (\bar{\sigma}_r \bar{r} w'_m w'_n + \frac{\bar{\sigma}_\theta}{\bar{r}} w_m w_n) d\bar{r} \Bigg\} (q_{mc} q_{nc} + q_{ms} q_{ns}) \Bigg\}_k \\
&\qquad + \frac{1}{2}\sum_m \sum_n \int_0^1 (U''_m U''_n a_m a_n + V''_m V''_n b_m b_n) d\bar{z}
\end{aligned} \tag{16}$$

Where, $\overline{\Omega}$ , is the non-dimensional rotor speed, and $\beta_i$ is the disk to shaft flexural rigidity ratio. The governing equations of motion can be derived by direct application of Lagrange's equation to the above kinetic and potential energy expressions in terms of $a_i$ and $b_i$ $(i = 1,......., M_s)$, $q_{si}$ and $q_{ci}$ $(i = 1,......., N_d * M_d)$ generalized coordinates, where $M_s$, $M_d$, and $N_d$ are the number of considered shaft modes, disk modes, and number of disks attached to the shaft, respectively.
The resulting equation of motion can be written in the well known matrix form:

$$[M]\{\ddot{q}\} + [C]\{\dot{q}\} + [K]\{q\} = \{0\} \tag{17}$$

Where $[M]$, $[C]$ and $[K]$ are the mass, gyroscopic and stiffness matrices, respectively. Details of these matrices are given in [15]. A first order system of equations can be formulated as:

$$[A]\{\dot{P}\} + [B]\{P\} = \{0\} \tag{18}$$

Where $[A] = \begin{bmatrix} [M] & [C] \\ [0] & [M] \end{bmatrix}$ and $[B] = \begin{bmatrix} [0] & [K] \\ [-M] & [0] \end{bmatrix}$

he corresponding eigenvalue problem is obtained, which can be solved to give the natural frequencies and mode shapes.

## EXPERIMENTAL MODAL ANALYSIS

The experimental study of vibration has contributed to understand and control this phenomenon, encountered in practice. Vibration testing is carried out for two objectives: First, to determine the vibration response levels during operation of the machine or structure under study, second, to verify theoretical models and prediction by measuring the vibration response of the structure or component under the influence of a known excitation. The second type of test is generally made under controlled condition to yield accurate and detailed information. This type of test is known as Experimental Modal Analysis (EMA), and has been used in this work to determine the vibration characteristics of a multiple flexible disk-flexible shaft system. The experimentally obtained results are used to verify the suggested earlier theoretical model. This work involves data acquisition, signal processing, and subsequent modal parameter extraction from the obtained Frequency Response Functions (FRF). The stationary flexible shaft carrying multiple flexible disk configurations, shown in figure 1, have been tested. The flexible disks have uniformly distributed stiffness and mass, and rigidly attached to the shaft, which is considered as a slender beam with axi-symmetric cross-section and uniformly distributed mass and stiffness.

**Experimental setup:**
Figure 3, shows a schematic diagram of the experimental setup, used in the present work, where one can identify the following main components:

1. Source of excitation, to provide a known input force to the structure. The impact test has been adopted using an impact hammer, which has a built in load cell to capture the induced impulse force.
2. Accelerometer: A piezoelectric accelerometer has been used to convert the mechanical motion of the structure into an electrical signal. Wax has been used to fix the accelerometer to the surface of the tested structure, at a location away from the nodes of its vibration modes.
3. Charge Amplifier: The amplifier is necessary to boost the very small electrical charge, generated by the accelerometer into a signal, strong enough to be fed to the data acquisition card.
4. Personal Computer with data acquisition card and signal processing software. The data acquisition card is to convert the captured analog signal to a digital signal, and the signal processing software to analyze this data, in order to obtain the Frequency Response Function (FRF), which will give the desired modal parameters i.e., frequency, damping and mode shapes. The LabView software was used for this purpose.

The captured signals from the accelerometer and hammer are in the time domain. The desired modal properties are obtained from the FRF, which is the ratio of the response to the excitation signals in the frequency domain.

$$H(\omega) = \frac{X(\omega)}{F(\omega)} \tag{19}$$

The obtained complex Frequency Response Function (FRF) is represented in term of its magnitude and phase. At resonance, the magnitude of FRF rapidly approach a sharp maximum value, and the phase shifts by $180^o$ as the frequency sweeps through resonance, which corresponds to zero real part.

To build confidence in the experimental setup, and subsequent modal parameter extraction from the FRF, it was first applied to determine the natural frequencies of a cantilever beam, free-free beam, circular solid disk with free boundaries, and square plate free at all sides. The obtained frequencies were found to agree with the available theoretical frequencies as shown in table 1.
Table 1. Theoretical and experimental natural frequencies of the lowest four modes measured in (Hz) for Free-Free beam, cantilevered beam, solid circular disk, and square plate are given below [16].

| Tested member / Frequency | Cantilever beam | | Free-Free beam | | Circular disk | | Square plate | |
|---|---|---|---|---|---|---|---|---|
| | Theo. | Exp. | Theo. | Exp. | Theo. | Exp. | Theo. | Exp. |
| 1st | 33.04 | 32 | 158.4 | 165.5 | 140.7 | 139.8 | 133 | 130.1 |
| 2nd | 207.1 | 199 | 436.6 | 451 | 243.2 | 241.8 | 195 | 193 |
| 3rd | 579.8 | 586.2 | 855.9 | 869 | 327.7 | 322.9 | 227 | 260 |
| 4th | 1136.3 | 1071.3 | 1414.9 | 1420 | 549.8 | 563.2 | 341 | 352.3 |

Once confidence is built in the employed experimental procedure, one can proceed to test the multiple flexible disk-flexible shaft system, as discussed in the following section.

## RESULTS AND DISCUSSION:

The described earlier Theoretical and Experimental Modal Analysis (TMA, and EMA) are applied to determine the natural frequencies of the following shaft-disk systems: A simply supported shaft carrying one flexible disk at $\bar{z}_1 = 0.5,$; A simply supported shaft carrying two identical flexible disks at $\bar{z}_1 = 0.2278, \quad and \quad \bar{z}_2 = 0.5$; A simply supported shaft carrying three identical flexible disks at $\bar{z}_1 = 0.2278, \quad \bar{z}_2 = 0.5, \quad and \quad \bar{z}_3 = 0.768$; A cantilever shaft carrying one flexible disk at $\bar{z}_1 = 1.0$; A cantilever shaft carrying two identical flexible disks at $\bar{z}_1 = 0.433 \quad and \quad \bar{z}_2 = 0.7274$; A cantilever shaft carrying three identical flexible disks at $\bar{z}_1 = 0.163, \quad \bar{z}_2 = 0.433, \quad and \quad \bar{z}_3 = 0.7274$.

The geometric and material properties of the used shaft and disks are as follows:

$h_d = 5\,\text{mm}, \; \text{R}_\text{d} = 127.5\,\text{mm}, \; \text{r}_\text{s} = 10\text{mm}, \; \rho_\text{d} = \rho_s = 7800\,\frac{\text{kg}}{\text{m}^3}, \; \text{E}_\text{d} = E_s = 200\,\text{Gpa}$

$\nu_\text{d} = \nu_s = 0.3$; $L_{\text{cantilever shaft}}$ = 765 mm.; $L_{\text{simply supported shaft}}$=785 mm.

The first five natural frequencies, obtained from Theoretical Modal Analysis (TMA) and Experimental Modal Analysis (EMA) for the considered shaft-disk configurations are given in table 2. The magnitude of the obtained Frequency Response Functions (FRF) for the simply supported shaft-disk and cantilever shaft-disk systems are shown in figures 4 and figure 5, respectively. The presented results in Table 2 show acceptable agreement between theoretical (TMA) and experimental (EMA) results, which provides the confidence to use the adopted theoretical approach to predict the natural frequencies of the rotating multiple flexible disks on a flexible shaft. The obtained theoretical results for simply supported and fixed-free shafts, with three identical flexible disks, are shown in figures 5, 6, and figures 9, 10, respectively. The coupling effects between shaft and disk modes are clearly demonstrated in the presented results. This coupling is strongly influenced by the bending rigidity ratio $\beta$. Figure 5-a, presents the non-dimensional coupled frequencies as a function of non-dimensional rotor speed, for of a simply supported shaft carrying three identical flexible disks, with bending rigidity ratio of 0.1. From the presented results, one can see that the first and second shaft modes strongly interact with disk modes. However, for higher bending rigidity ratio, $\beta = 10$, for example, the frequency of disk modes is higher than in the case with $\beta = 0.1$, and coupling takes place between the same disk modes and higher shaft modes, as seen in figure 5-b. Similar results for the fixed-free shaft with three flexible disks are shown in figures 7-a and 7-b.

As mentioned earlier, the considered disks are identical, therefore, they have the same uncoupled frequencies. But when these same disks are attached at different spanwise positions of the flexible shaft, the same modes of the same disks are influenced by shaft modes differently, which results in different coupled frequencies of the same disks, giving rise to a number of close frequencies in the coupling region, which can be seen in the presented results, figure 5 and 7.

On other hand, the dynamic coupling between the shaft and disk modes has been investigated as a function of flexural rigidity ratio $\beta$. The effect of on the uncoupled frequencies of the considered multiple disk shaft system is shown in figures 6 and 8, for simply supported and fixed-free shafts, respectively. The results are presented for two non-dimensional rotor speed of 0.0 and 10.0.

## CONCLUSIONS

The coupled disk-shaft frequencies of a multiple disk-shaft system are determined from a proposed theoretical model, and correlated with similar results obtained from experiment. The assumed mode method is used to formulate equations of motion for any number of flexible disks attached to a flexible shaft. On the other hand, a single input single output approach is used, with an impact hammer to excite the system, and a piezoelectric accelerometer to measure the response, and frequency information of the tested system are obtained from the generated Frequency Response Function. Further steps are to be taken as a follow up on the presented work: First, to test the system while rotating, and second, to apply a global curve fitting method on the experimental results to extract various modal parameters, i.e., modal damping and mode shapes besides the natural frequencies.

Table 2. Theoretical and experimental natural frequencies measured in (Hz) for non-rotating flexible shaft with multiple flexible disks.

| Shaft Configuration / Natural Frequency | | Simply Supported shaft | | | Cantilever Shaft | | |
|---|---|---|---|---|---|---|---|
| | | 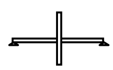 | 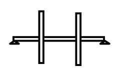 | 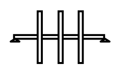 | 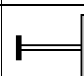 | 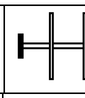 | 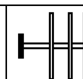 |
| 1st | TMA | 36.5 | 31.1 | 27.7 | 10.5 | 13.6 | 13.6 |
| | EMA | 35 | 29.8 | 27 | 10.5 | 13.5 | 13 |
| 2nd | TMA | 157.5 | 126.7 | 102.1 | 87.9 | 77.3 | 73.7 |
| | EMA | 142.5 | 117.5 | 97.3 | 90.1 | 80 | 76.3 |
| 3rd | TMA | 310 | 202.6 | 191.9 | 221.1 | 177.2 | 157 |
| | EMA | 282.2 | 189.2 | 178.6 | 248.3 | 170.1 | 147.02 |
| 4th | TMA | 441.03 | 262.2 | 205.9 | 352.4 | 255.4 | 246.8 |
| | EMA | 448.5 | 234.4 | 209.3 | 356.3 | 233 | 232.9 |
| 5th | TMA | 688.02 | 368.4 | 256.6 | 608.4 | 305.4 | 264.2 |
| | EMA | 694.4 | 355.5 | 232.5 | 652.2 | 281 | 251.9 |

## REFERENCES:


1. Chong-Won Lee and Sang-Bok Chun, Vibration analysis of a rotor with multiple flexible disks using assumed mode method, Journal of vibration and acoustics, 120; 87-94, 1998.
2. S.B. Chun and C.W. Lee, Vibration analysis of shaft-bladed disk system by using substructure synthesis and assumed mode method, Journal of sound and vibration, 189(5), 587-608, 1996.
3. Shahab A. S.and Thomas J., Coupling effect of disk flexibility on the dynamic behavior of multi disk-shaft system, Journal of sound and vibration, 114(3), 435-446, 1987.

4. Jia H. S., Chun S.B. and Lee C.W., Evaluation of the longitudinal coupled vibration in rotating, flexible disk/spindle system, Journal of sound and vibration, 208(2),175-187, 1997.
5. Chong-Won Lee and Jong Ham, Mode identification for rotating rigid shaft with flexible disks by mode splits, Journal of sound and vibration, 225(3), 425-446, 1999.
6. Shen I.Y. and Ku C.P.R., A Nonclassical vibration analysis of a multiple rotating disk and spindle assembly, Journal of Applied Mechanics, 64, 165-174,1997.
7. Wu F. and Flowers G.T., A transfer matrix technique for evaluating the natural frequencies and critical speeds of a rotor with multiple flexible disks, Journal of vibration and acoustics, 114, 242-248, 1992.
8. Lee C. W., Jia H.S., Kim C.S. and Chun S.B., Tuning of simulated natural frequencies for a flexible shaft-multiple flexible disk system, Journal of sound and vibration, 207(4), 435-451, 1997.
9. Shen Jr-Yi, Chaw-Wu Tseng and Shen I.Y., Vibration of rotating disk/spindle system with flexible housing/stator assemblies, Journal of sound and vibration, 271,; 725-756, 2004.
10. Jang G.H., Lee S.H. and Jung M.S., Free vibration analysis of a spinning flexible disk-spindle system supported by ball bearing and flexible shaft using the finite element method and substructure synthesis, Journal of sound and vibration, 251(1), 59-78, 2002.
11. Seungchul Lim, Finite element analysis of flexural vibration in hard disk drive spindle system, Journal of sound and vibration, 233(4), 601-616,.2000.
12. Khader N. and Masoud S., Vibration of mistuned bladed disks supported by flexible continuous shaft, Journal of sound and vibration, 149(3), 471-488, 1991.
13. Khader N. and Loewy R.G., Shaft flexibility effect on the forced response of a bladed disk assembly, Journal of sound and vibration, 139(3), 469-485.1990.
14. Loewy R.G. and Khader N., Structural dynamics of rotating bladed-disk assemblies coupled with flexible shaft motion, AIAA Journal, 22, 1319-1327, 1984.
15. Atoum Ali, Modal analysis of flexible disks on a flexible shaft, MSc Thesis, Department of Mechanical Engineering, Jordan University of Science & Technology, May 2006.
16. WEAVER W. JR., Vibration problems in engineering, John Wiley and sons, 1990.

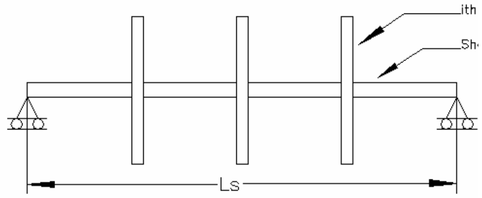


a) Multiple disks on a simply supported shaft

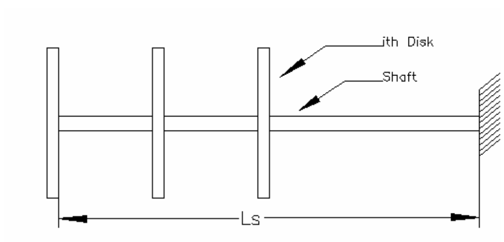


b) Multiple disks on a fixed-free shaft

Figure 1: Multiple flexible disks on a flexible shaft.

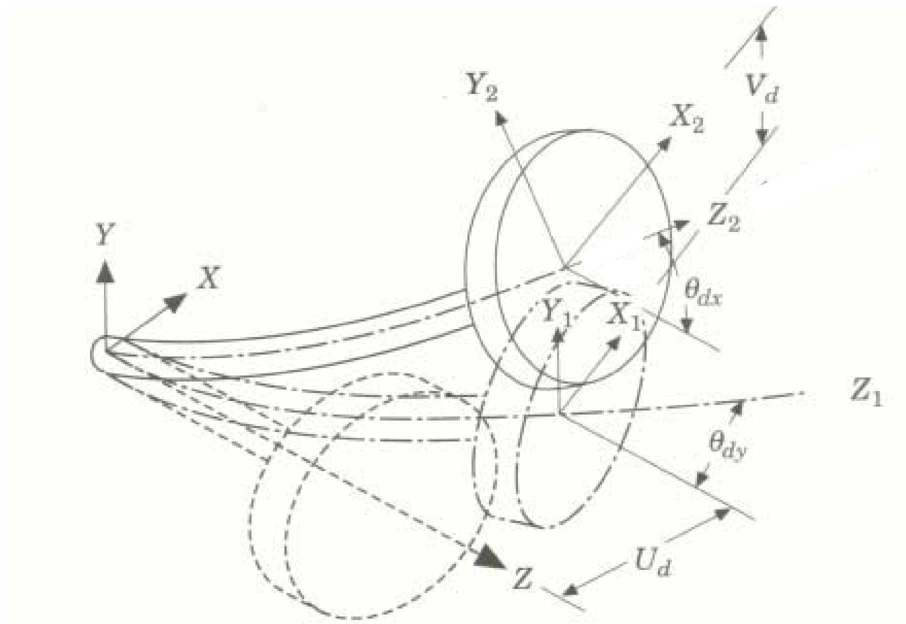


Figure 2: Coordinate systems used to describe Flexible disk and Shaft deformations.

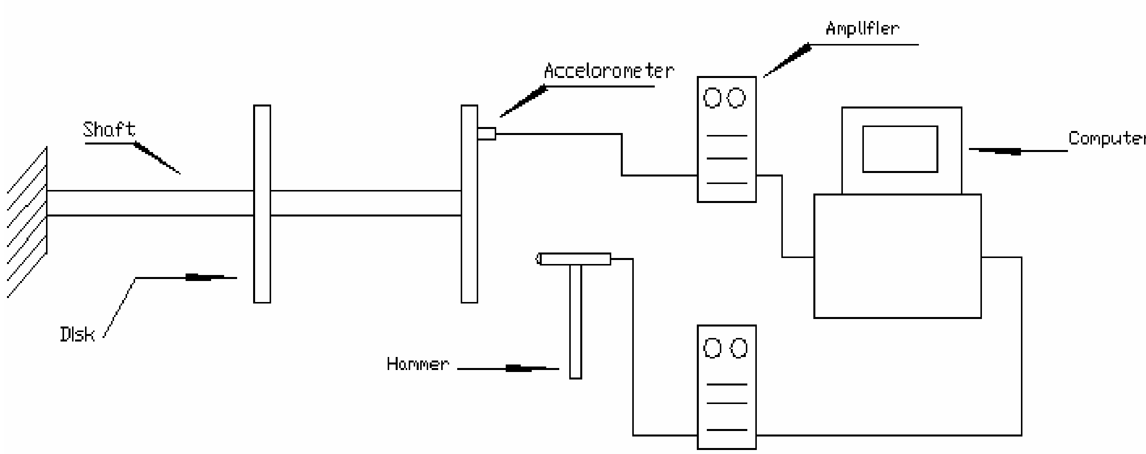


Figure 3: Experimental setup

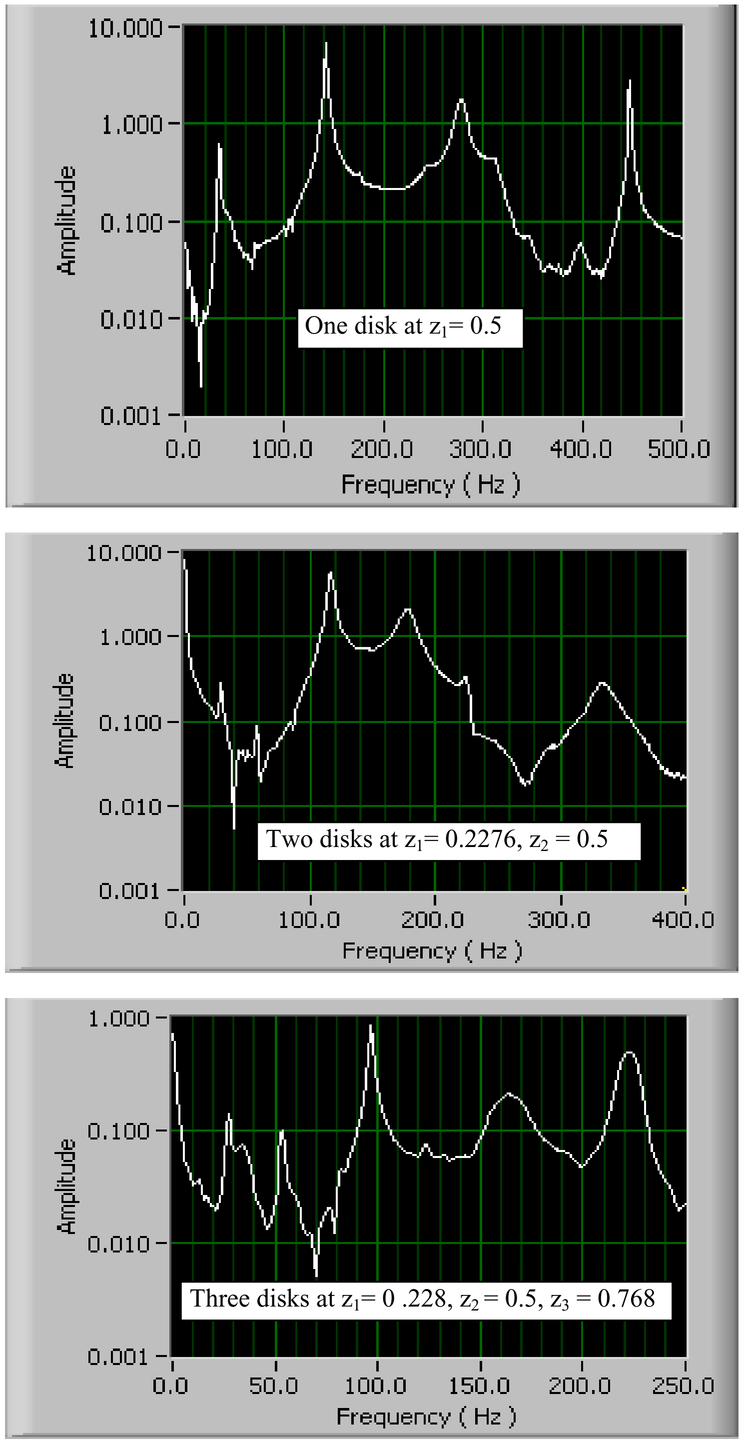


Figure 4: Magnitude of the FRF for a simply supported shaft with, one, two, and three disks.

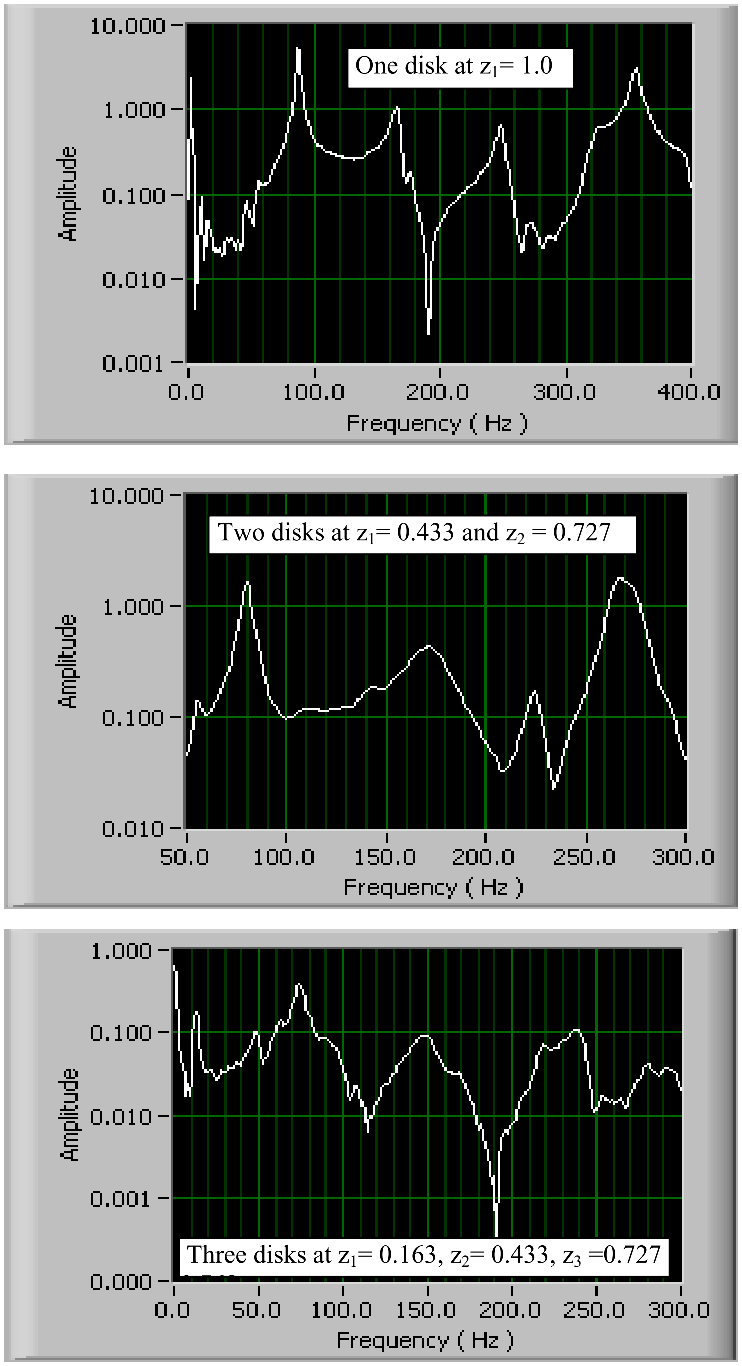


Figure 5: Magnitude of the FRF for a cantilever shaft with one, two, and three disks.

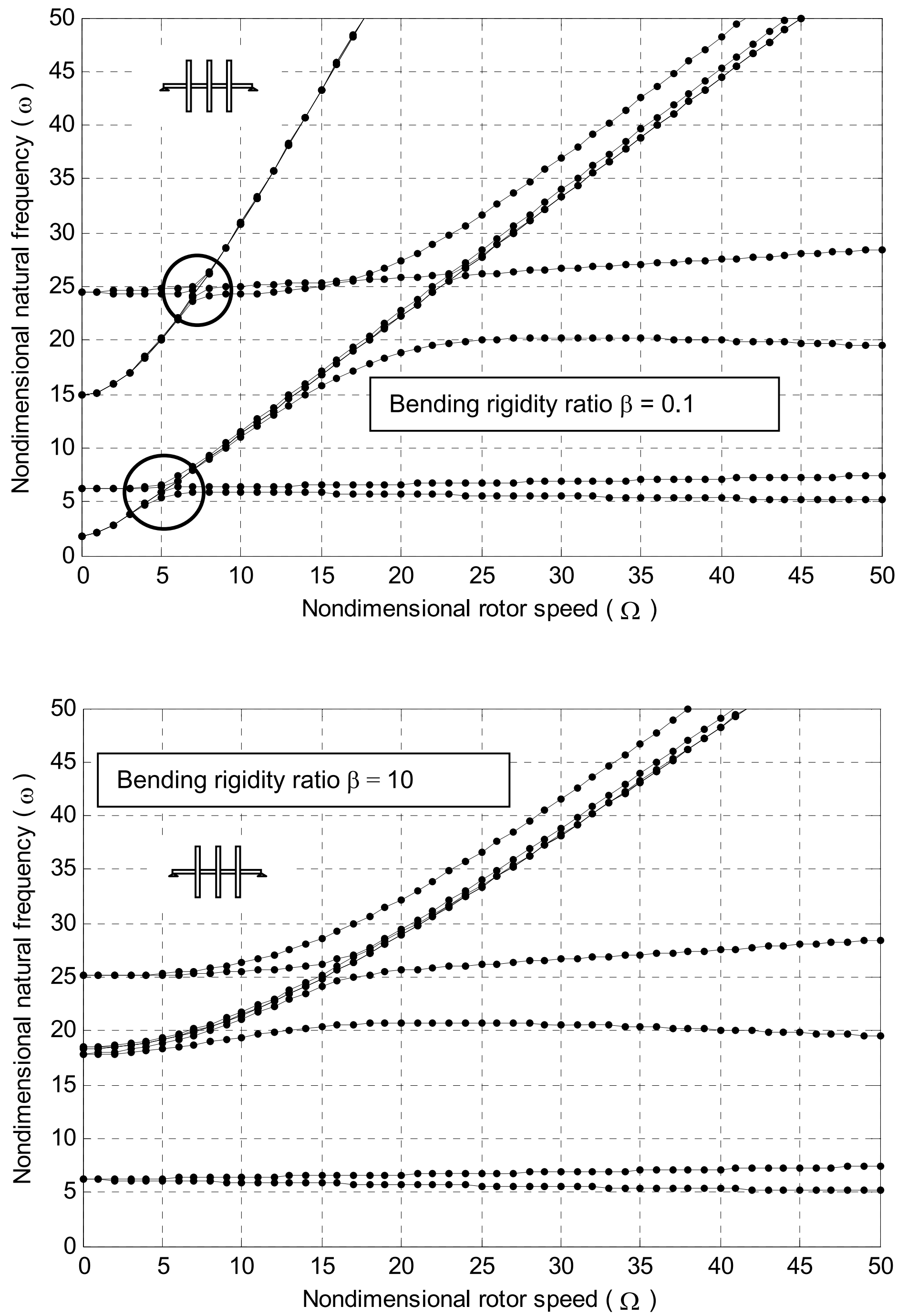


Figure 6: Non-dimensional coupled natural frequency versus non-dimensional rotor speed for a simply supported shaft with three flexible disks.

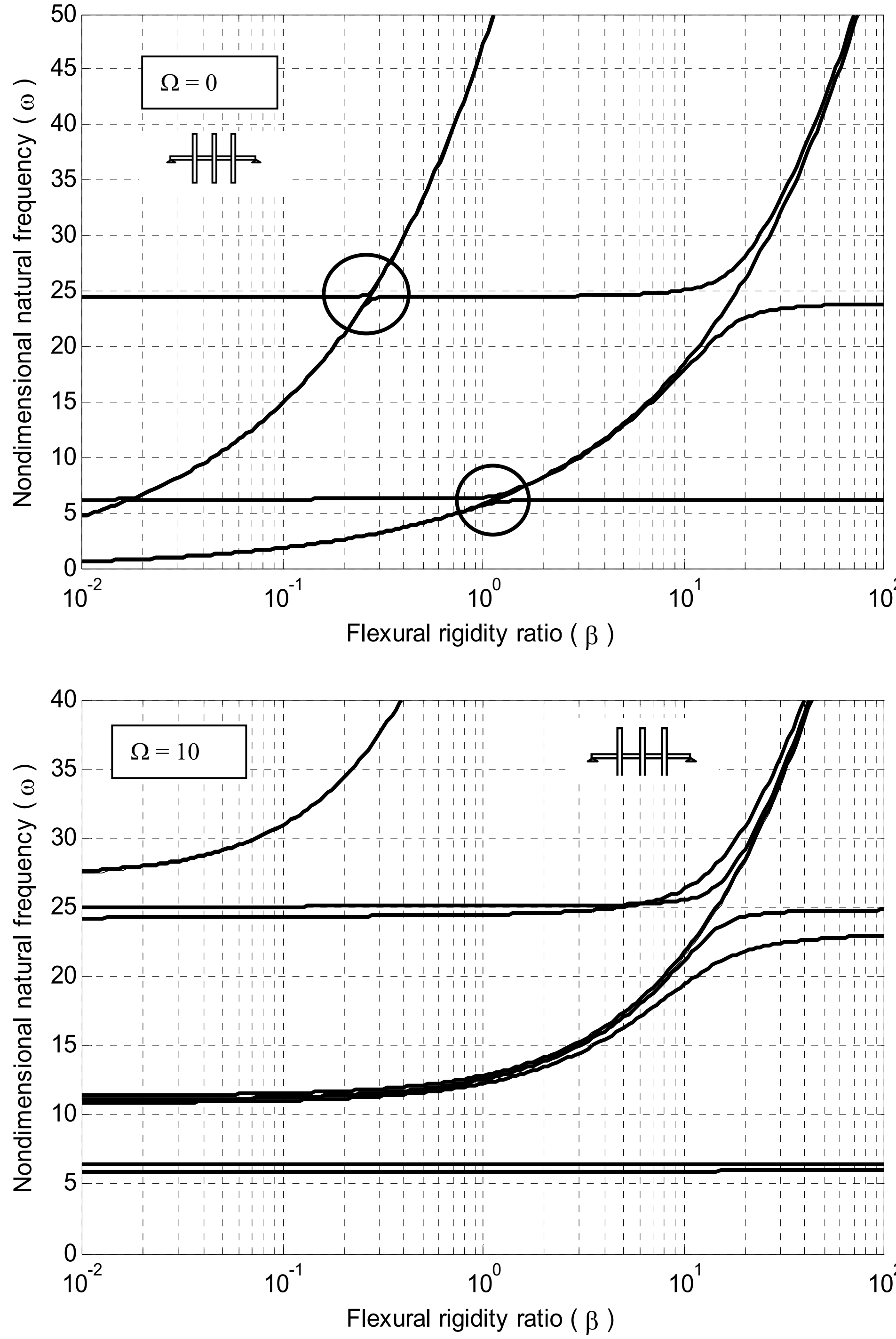


Figure 7: Non-dimensional coupled natural frequency versus flexural rigidity ratio for a simply supported shaft with three flexible disks

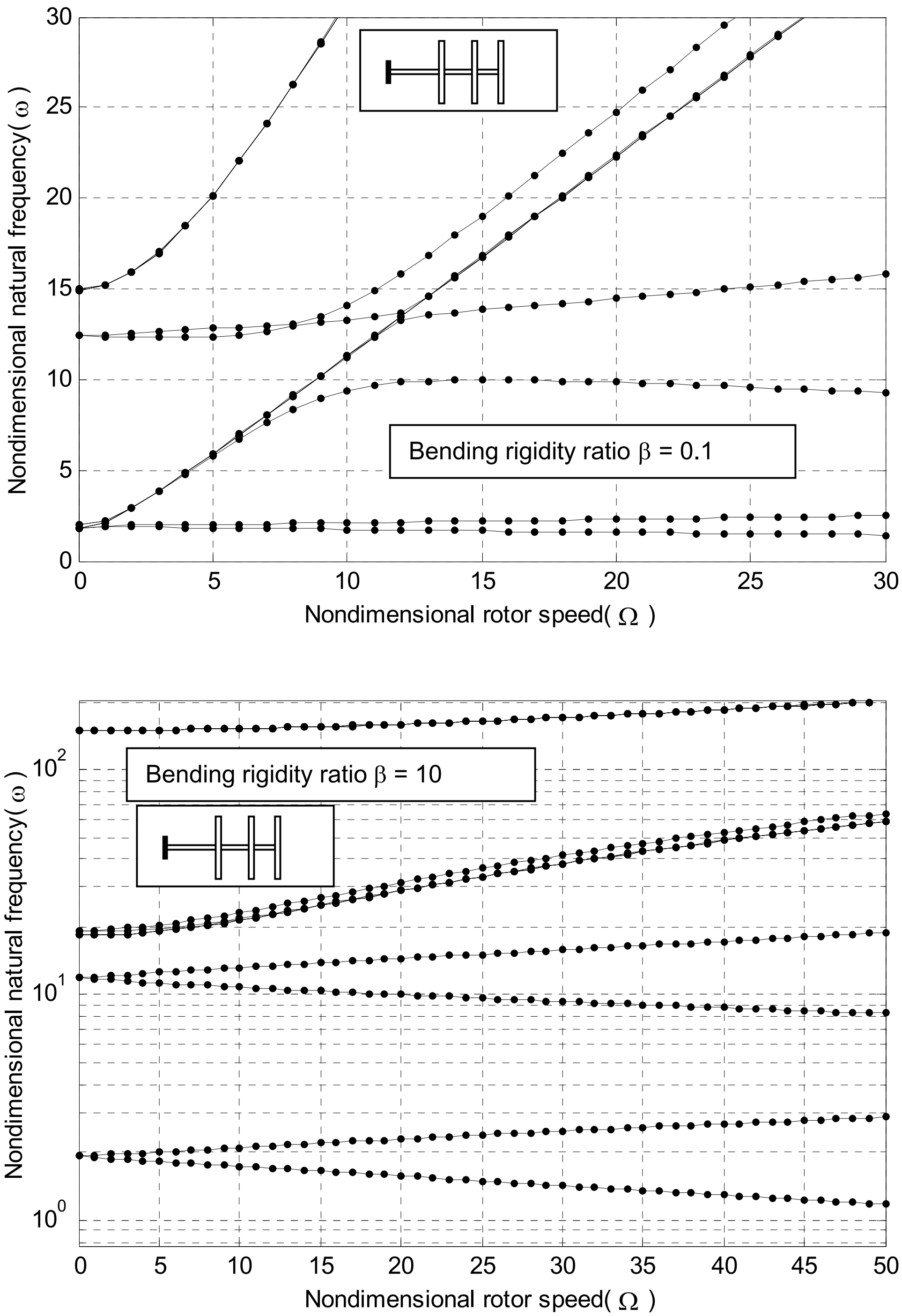


Figure 8: Non-dimensional coupled natural frequency versus non-dimensional rotor speed for a clamped free shaft with three flexible disks

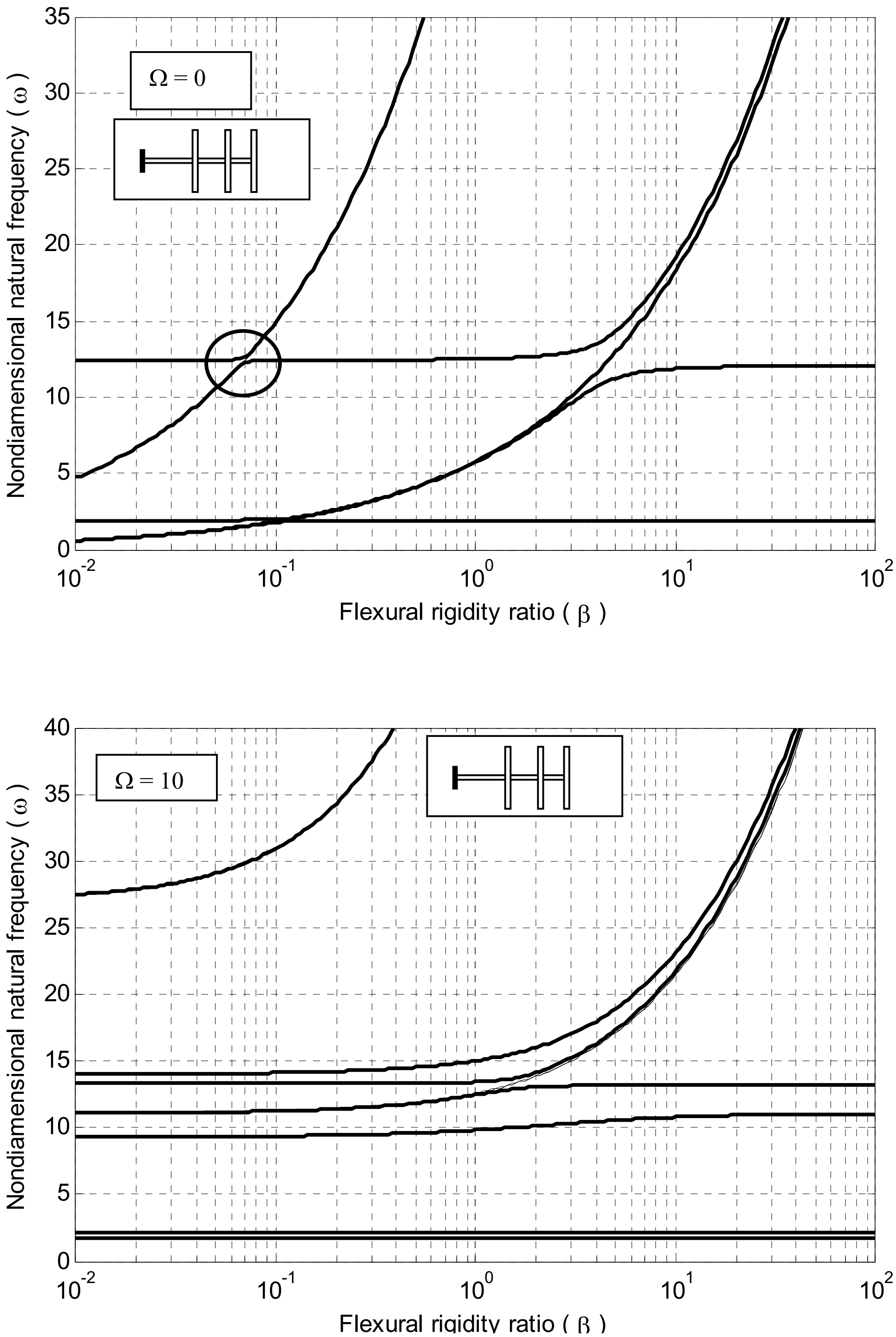


Figure 9: Non-dimensional coupled natural frequency versus flexural rigidity ratio for a clamped free shaft with three flexible disks